

Abb.: Farbreaktion nach Emerson

1: 4-Aminophenazon

2: 4-(*N,N*-Dimethylamino)phenazon

K: Kontrolle

**Tabelle: Trivial- und Handelsnamen der untersuchten Verbindungen**

4-Aminophenazon (1)	4- <i>N,N</i> -Dimethylaminophenazon (2)
4-AAP	Aminophenazon(e)
4-Aminoantipyrene	Aminopyrine
Aminoantipyrin(e)	Amidopyrin(e)
4-Aminoantipyrine	Amidazophen(e)
Ampyrone	Amidofebrin
Metapirazone	Amidofen

### Experimenteller Teil

Durchführung nach Emerson (1943): 15 mg Phenol werden in 10 ml H<sub>2</sub>O gelöst und mit 3 Tropfen einer NH<sub>4</sub>OH-Lsg. (*c* = 6 mol/l) versetzt. Die Lösung wird in zwei gleiche Teile geteilt, von denen der eine mit 2 Tropfen einer 2%igen Aminophenazon-Lsg. versetzt wird und der andere als Kontrolle dient. Beide Lösungen werden mit 3 Tropfen einer 8%igen K<sub>3</sub>[Fe(CN)<sub>6</sub>]-Lsg. versetzt.

### Literatur

- Eger K, Troschütz R, Roth HJ (2005) *Arzneistoffanalyse*, 5. Aufl., Deutscher Apotheker Verlag Stuttgart, S. 40.
- Emerson E (1943) The condensation of aminoantipyrine, part II. *J Org Chem* 8: 417–428.
- Emerson E, Kelly K (1948) The condensation of aminoantipyrine, part VI. *J Org Chem* 13: 532–534.
- Göber B, Surmann P (2005) *Arzneimittelkontrolle – Drug Control*, 1. Aufl., Wissenschaftliche Verlagsgesellschaft mbH Stuttgart, S. 446–449.

Programa de Pós-Graduação em Ciências Farmacêuticas, Departamento de Controle e Produção de Medicamentos<sup>1</sup>, Faculdade de Farmácia, Departamento de Mineralogia e Petrologia<sup>2</sup>, Instituto de Geociências, Universidade Federal do Rio Grande do Sul, Porto Alegre, Brasil

### Characterization of different samples of quercetin in solid-state: indication of polymorphism occurrence

G. S. BORGHETTI<sup>1</sup>, I. M. COSTA<sup>1</sup>, P. R. PETROVICK<sup>1</sup>, V. P. PEREIRA<sup>2</sup>, V. L. BASSANI<sup>1</sup>

Received August 24, 2005, accepted January 23, 2006

Prof. Dra. Valquiria Linck Bassani, Departamento de Controle e Produção de Medicamentos, Faculdade de Farmácia, Universidade Federal do Rio Grande do Sul, N° 2752, Avenida Ipiranga, Porto Alegre, 90610-000, Brasil  
valqui@farmacia.ufrgs.br

*Pharmazie* 61: 802–804 (2006)

The present work was designed to compare four commercial samples of quercetin, three of them presenting pharmaceutical grade (QPGa, QPGb and QPGc) and the other one pro-analytical grade (QPA) by means of different techniques. Physical and chromatographic characterization of these samples shows different properties following its origin, especially a clear evidence of polymorphism occurrence.

Quercetin belongs to the flavonoid class and its biological activities have been described extensively (Murota and Terao 2003; Moskaug et al. 2004; Okamoto 2005). However, few studies concerning solid-state properties of quercetin have been reported (Heneczowski et al. 2001; Costa et al. 2002; Olejniczak and Potrzebowski 2004; Costa 2005). In the present work, three samples of quercetin presenting pharmaceutical grade were compared to a pro-analytical grade sample by means of Liquid Chromatography (LC), Ultraviolet Spectroscopy (UV), Infrared Spectroscopy (IR), Differential Scanning Calorimetry (DSC), X-Ray Powder Diffraction Analysis (XRPD), Scanning Electron Microscopy (SEM) techniques and aqueous solubility determination.

The LC profile of all quercetin samples showed peaks with very similar retention times (6.8 min). Considering the peak area of QPA as 100%, the lower concentration of QPGa (92.0% ± 0.4) and QPGc (93.6% ± 1.4) samples could be due to the residual water content. The concentration higher than 100% in QPGb (105.5% ± 0.4) sample could indicate the presence of impurities or lower residual water content than QPA.

For all samples coincident UV spectra were observed. Their maximum absorption wavelength values (256 and 372 nm) are in accordance with the spectra reported in the literature (Mabry et al. 1970; Budavari 1996).

Coincident IR spectra of QPA and QPGa samples were obtained, both presenting the main characteristic bands of the molecule: at 3408.6 cm<sup>-1</sup> (–OH deformation), 900 and 675 cm<sup>-1</sup> (–CH deformation), 1260 and 1000 cm<sup>-1</sup> (–CO deformation), 1150–1085 cm<sup>-1</sup> (C–O–C deforma-

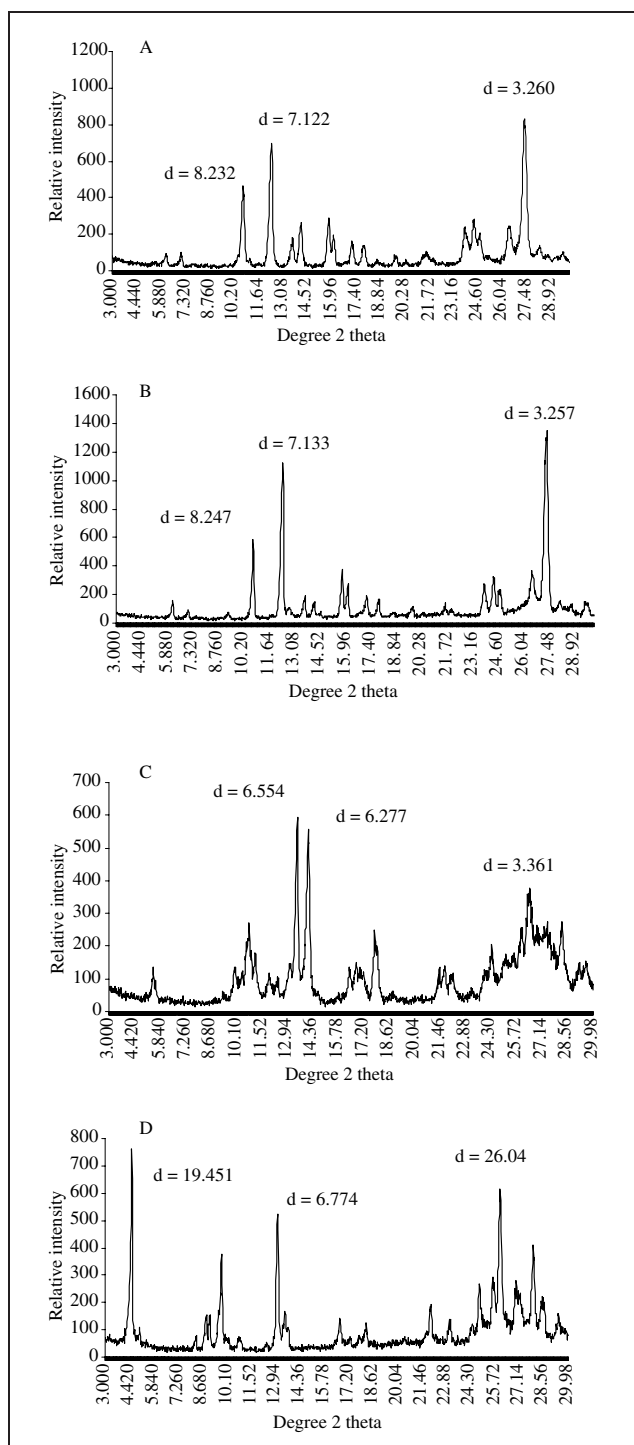


Fig. 1: XRPD analysis of quercetin samples from different suppliers (A) QPA, (B) QPGa, (C) QPGb and (D) QPGc

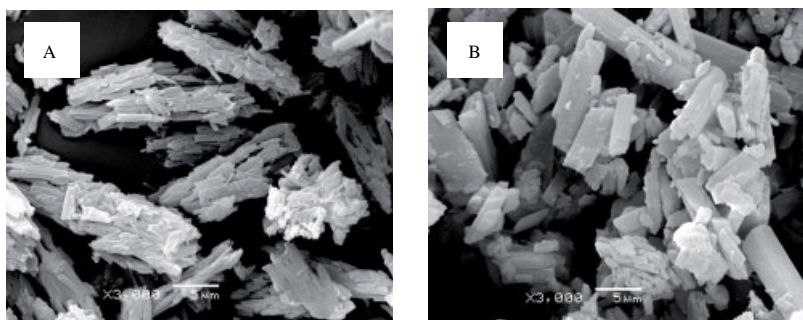
tion) and  $1666.7\text{ cm}^{-1}$  ( $=\text{CO}$  stretching). The IR spectra of QPGb and QPGc samples also were coincident, but they are not in accordance with the spectra related in the literature (Pouchert 1991). In this case, the band relative to  $-\text{OH}$  deformation ( $3408.6\text{ cm}^{-1}$ ) presents different shape when compared with the IR spectra of QPA and QPGa. The band correspondent to the  $=\text{CO}$  stretching ( $1666.7\text{ cm}^{-1}$ ) is in the same position in all recorded spectra. The main difference is found in the position and shape of the bands related to the  $-\text{CO}$  deformation ( $1260$  and  $1000\text{ cm}^{-1}$ ). Additionally some differences in the bands related to the  $-\text{CH}$  deformation ( $900$  and  $675\text{ cm}^{-1}$ ) were observed. These differences could be related to the presence of hydration water as well as differences between their crystal lattices.

In DSC analysis, the first endothermic event observed for QPA and QPGa samples corresponds to the loss of the bounded water. QPA and QPGa samples presented onset temperature values for this event of  $114.20^\circ\text{C}$  and  $85.61^\circ\text{C}$ , respectively. This peak is not present in the QPGb sample and, in the case of QPGc sample, such a peak is displaced to lower temperatures compared to QPA and QPGa samples ( $31.26^\circ\text{C}$ ), suggesting that this peak cannot be related to the loss of bounded water. In the same way, the peak corresponding to the melting point of the quercetin presented different onset temperature values for all samples. QPA, QPGa and QPGc samples presented onset temperature values of  $322.57^\circ\text{C}$ ,  $318.96^\circ\text{C}$  and  $315.31^\circ\text{C}$ , respectively. The onset temperature differences for QPA and QPGa samples, upon to the presence of an exothermic signal on about  $200^\circ\text{C}$  in QPGa, which was no detected in the thermogram of QPA, could suggest differences in crystal lattice, size or morphology of particles of both samples. QPGb sample, on the other hand, presented two endothermic peaks between  $314$  and  $320^\circ\text{C}$ : the first one with an onset temperature of  $314.54^\circ\text{C}$  (similar to the value observed for QPGc sample) and the other one with an onset temperature of  $319.86^\circ\text{C}$  (similar to the values observed for QPA and QPGa samples).

The XRPD analysis (Fig. 1) showed that QPA and QPGa samples present the same XRPD pattern and, consequently, identical crystal lattices. QPGb and QPGc samples, on the other hand, presented two different XRPD patterns. These results indicate the occurrence of three different polymorphic forms of quercetin. Distinct crystal lattices of QPGb and QPGc samples, when compared to QPA and QPGa, could explain the results observed in DSC analysis. Nevertheless, the results obtained in thermal analysis of QPA and QPGa samples cannot be explained by XRPD data.

The aqueous solubility values observed for QPGa, QPGb and QPGc samples were,  $1.69 \pm 0.02$ ,  $1.22 \pm 0.05$  and  $2.97 \pm 0.27\text{ }\mu\text{g/mL}$ , respectively. These values were higher than that observed for QPA ( $0.48 \pm 0.03\text{ }\mu\text{g/mL}$ ). The dif-

Fig. 2: Photomicrographs of quercetin samples (A) QPA and (B) QPGa



ference in aqueous solubilities among QPA, QPGb and QPGc samples is probably due to their distinct crystal lattices. Nevertheless, comparing QPA and QPGa samples, the aqueous solubility differences could be caused by different particle morphology.

Effectively, the SEM photomicrographs of QPA and QPGa samples demonstrated the existence of differences in particle morphology and size between both samples (Fig. 2). In the QPA sample it is possible to observe the presence of euhedral particles (with size between 2 and 4  $\mu\text{m}$ ), whereas the QPGa sample is composed of particles presenting subhedral shape (the majority form is columnar and with size between 3 and 5  $\mu\text{m}$ ). The DSC analysis response and aqueous solubility of QPA and QPGa samples can be related to the particle morphology and particle size.

Taken together, physical and chromatographic characterization of four different commercial samples of quercetin shows different properties following its origin, which is a clear evidence of polymorphism occurrence.

## Experimental

Quercetin pharmaceutical grade were purchased from DEG<sup>®</sup> (QPGa), Galena<sup>®</sup> (QPGb) and SPFarma<sup>®</sup> (QPGc) (Brazil) and quercetin pro-analysis grade (QPA) was obtained from Sigma<sup>®</sup> (USA). Liquid chromatography was performed using the method developed and validated by Webber (2003), in a Shimadzu LC-10A equipment and a Shimadzu CLC-ODS (M) RP 18.5  $\mu\text{m}$  (250  $\times$  4 mm i.d.) column. Each sample was analysed in triplicate. The spectral analysis (200 to 500 nm) was performed in a Hewlett-Packard 8452A Scanning Spectrophotometer UV-VIS, using a methanolic solution containing 16  $\mu\text{g}/\text{mL}$  of each sample, in quartz cell and path length of 1 cm. The IR spectra (4000 to 400  $\text{cm}^{-1}$ ) were obtained in a Shimadzu DR-8001 IR Spectrophotometer in KBr discs, using a resolution of 4  $\text{cm}^{-1}$  and 40 accumulations. For differential scanning calorimetric analysis, samples corresponding to around 1 to 2 mg were placed in aluminum pans and crimped. The analysis were carried out in a Shimadzu DSC-60 equipment. The operating conditions were 10  $^{\circ}\text{C} \cdot \text{min}^{-1}$  of heating rate, from 25 up to 350  $^{\circ}\text{C}$ ,  $\text{N}_2$  dynamic atmosphere, 50  $\text{mL} \cdot \text{min}^{-1}$  of flow. Temperature calibration was performed using Indium and Zinc. Diffractograms were obtained at room temperature in a Siemens D-5000 X-ray diffractometer. The setting parameters were Ni filtered  $\text{Cu K}\alpha$  radiation ( $\lambda = 1.5418 \text{ \AA}$ ), high voltage of 40 kV, tube current of 30 mA, step of 0.02 $^{\circ}$   $2\theta^{\circ}$  and angular range of  $2^{\circ} < 2\theta < 72^{\circ}$ . Aqueous solubility determination was carried out by adding an excess amount of sample (6 mM) to 10 mL of water. The suspensions resulting were stirred for 24 h, at 37  $^{\circ}\text{C}$ . Samples were filtered and the quercetin content in the solutions was assayed by ultraviolet spectroscopy at 372 nm. Each sample was analysed in triplicate. The scanning electron microscopy analysis was performed in a JSM-6060 SEM, using a voltage of 20 kV. Samples were analyzed after gold sputtering.

Acknowledgement: This research was supported by the Brazilian Government (CAPES, CNPq and FAPERGS).

## References

- Budavari S (ed.) (1996) The Merck Index: an encyclopedia of chemicals, drugs and biologicals. 12<sup>th</sup> ed., Whitehouse Station.
- Costa EM, Barbosa-Filho JM, Nascimento TG, Macedo RO (2002) Thermal characterization of the quercetin and rutin flavonoids. *Thermochimica Acta* 392–393: 79–84.
- Costa IM (2005) Estudo de pré-formulação com o composto polifenólico quercetina. M.Sc. Thesis (Master in Pharmaceutical Sciences) – Programa de Pós-Graduação em Ciências Farmacêuticas, Faculdade de Farmácia, Universidade Federal do Rio Grande do Sul, Porto Alegre.
- Henczkowski M, Kopacz M, Nowak D, Kuzniar A (2001) Infrared spectrum analysis of some flavonoids. *Acta Pol Pharm* 58: 415–420.
- Mabry TJ, Markhan KR, Thomas MB (1970) The systematic identification of flavonoids. New York.
- Moskaug JO, Carlsen H, Myhrstad M, Blomhoff R (2004) Molecular imaging of the biological effects of quercetin and quercetin-rich foods. *Mech Ageing Dev* 125: 315–324.
- Murota K, Terao J (2003) Antioxidative flavonoid quercetin: implication of its intestinal absorption and metabolism. *Arch Biochem Biophys* 417: 12–17.
- Okamoto T (2005) Safety of quercetin for clinical application (Review). *Int J Mol Med* 16: 275–278.

Olejniczak S, Potrzebowski MJ (2004) Solid state NMR studies and density functional theory (DFT) calculations of conformers of quercetin. *Org Biomol Chem* 2: 2315–2322.

Pouchert CJ (ed.) (1991) The Aldrich Library of Infrared Spectra. 3<sup>rd</sup> ed., Wisconsin.

Webber C (2003) Avaliação do perfil de penetração cutânea da quercetina. M.Sc. Thesis (Master in Pharmaceutical Sciences) – Programa de Pós-Graduação em Ciências Farmacêuticas, Faculdade de Farmácia, Universidade Federal do Rio Grande do Sul, Porto Alegre.